Spin switching in semiconductor quantum dots through spin-orbit coupling

Manuel Valín-Rodríguez, Antonio Puente, and Llorenç Serra
Departament de Física, Universitat de les Illes Balears, E-07071 Palma de Mallorca, Spain

Enrico Lipparini
Dipartimento di Fisica, Università di Trento, and INFM Zezione di Trento, I-38050 Povo, Italy
(Received 19 June 2002; published 1 October 2002)

The spin-orbit coupling influences the total spin of semiconductor quantum dots. We analyze the theoretical prediction for the combined effects of spin-orbit coupling, weak vertical magnetic fields and deformation of the dot. Our results allow the characterization of the quantum dots as the spin switches, controllable with electric gates.

DOI: 10.1103/PhysRevB.66.165302 PACS number(s): 73.21.La

A technology based on the use of the electron spin, as opposed to the more traditional use of the electron charge, is emerging under the name of spintronics. Several spin-based electronic devices have already proved their importance, even at a commercial level, such as the spin-valve read heads. A review of the status of this incipient field can be found in Ref. 1.

The spin-orbit (SO) coupling is an essential mechanism for most spintronic devices, since it links the spin and the charge dynamics, opening the possibility of spin control through electric fields.[2] Indeed, recent experimental and theoretical investigations have shown that the SO coupling affects the charge transport and, more specifically, the conductance fluctuations of chaotic quantum dots in a parallel magnetic field.[3–5] It also affects the dot far-infrared absorption, introducing peculiar correlations between the charge and spin oscillating densities.[6] In this work we analyze the combined effects of SO coupling, weak vertical magnetic (B) fields, and spatial deformation in fixing the spin and other ground state properties of model semiconductor dots.

It will be shown that a sufficiently strong SO coupling can lead to spin inversion, with an alternating B dependence, similar to the observations from capacitance spectroscopy experiments of both vertical[7] and lateral quantum dots.[8] Since SO coupling is also active at low B's, this mechanism influences the weak-field regime and can provide an alternative interpretation to the one of Ciorga *et al.*,[8] which was based on calculations for high magnetic fields. In Ref. 8 an alternating up-down behavior of the dot spin was inferred from polarized-current spectroscopy and it was attributed to spin rearrangements induced by the Coulomb interaction.

We consider the SO coupling terms as reviewed by Voskoboynikov *et al.*[9] Assuming a two-dimensional system and the effective Hamiltonian formalism, the relevant Dresselhaus contribution for the standard (001) plane of GaAs reads

$$\mathcal{H}_D=\frac{\lambda_D}{\hbar}\sum_{i=1}^{N}\left[P_x\sigma_x-P_y\sigma_y\right]_i, \tag{1}$$

where the σ's are the Pauli matrices and $\mathbf{P}=-i\hbar\nabla+e/c\ \mathbf{A}$ represents the canonical momentum given in terms of the vector potential $\mathbf{A}$.[10] The Dresselhaus parameter λ_D is determined by the dot vertical width z_0 as[9] $\lambda_D\approx\gamma(\pi/z_0)^2$, with a material-specific constant γ that for GaAs is $\gamma=27.5$ eV Å^3.[11] A SO coupling of Rashba type[9] was also considered, although its contribution to the results for GaAs shown below turned out to be negligible.

Neglecting for the moment the Coulomb interaction the complete Hamiltonian reads $\mathcal{H}=\mathcal{H}_0+\mathcal{H}_D+\mathcal{H}_Z$, where $\mathcal{H}_0$ consists of the kinetic and confinement energies, i.e.,

$$\mathcal{H}_0=\sum_{i=1}^{N}\left[\frac{\mathbf{P}^2}{2m}+\frac{1}{2}m(\omega_x^2x^2+\omega_y^2y^2)\right]_i. \tag{2}$$

Note that the assumed anisotropic confinement will permit the modeling of dots with varying elliptical shapes. The Zeeman term $\mathcal{H}_Z$ depends on the total vertical spin S_z, the Bohr magneton μ_B, and the effective gyromagnetic factor g^*, which for bulk GaAs is -0.44. Namely, $\mathcal{H}_Z=g^*\mu_BBS_z$.

Assuming $\mathcal{H}_0\gg\mathcal{H}_D\gg\mathcal{H}_Z$ and expanding in powers of λ_D an analytic diagonalization to $O(\lambda_D^3)$ in spin space is possible with a unitary transformation[5] $\tilde{\mathcal{H}}=U_1^+\mathcal{H}U_1$, giving the transformed Hamiltonian

$$\tilde{\mathcal{H}}=\sum_{j=1}^{N}\left[\frac{\mathbf{P}^2}{2m}+\frac{1}{2}m(\omega_x^2x^2+\omega_y^2y^2)+\lambda_D^2\frac{m}{\hbar^3}L_z\sigma_z+\frac{1}{2}g^*\mu_BB\sigma_z\right]_j-N\lambda_D^2\frac{m}{\hbar^2}+O(\lambda_D^3), \tag{3}$$

where we have defined the *canonical* angular momentum operator $L_z=xP_y-yP_x$. Despite the spin diagonalization, the x and y degrees of freedom in Eq. (3) are still coupled through the vector potential in the kinetic energy and in L_z. With a second transformation each spin component can be recast in a separable form using the methods of Meyer, Kucar, and Cederbaum.[12] Specifically, defining $\hat{\mathcal{H}}_\eta=U_{2\eta}^+\tilde{\mathcal{H}}_\eta U_{2\eta}$, with $\eta=\uparrow,\downarrow$, we obtain

$$\hat{\mathcal{H}}_\eta=\sum_{j=1}^{N_\eta}\left[\frac{p_x^2}{2M_{1\eta}}+\frac{M_{1\eta}}{2}\Omega_{1\eta}^2x^2+\frac{p_y^2}{2M_{2\eta}}+\frac{M_{2\eta}}{2}\Omega_{2\eta}^2y^2+\frac{1}{2}g^*\mu_BBs_\eta\right]_j-N_\eta\lambda_D^2\frac{m}{\hbar^2}+O(\lambda_D^3), \tag{4}$$

where $s_\eta = \pm 1$ for $\eta = \uparrow, \downarrow$. Assuming, without loss of generality, $\omega_x \geqslant \omega_y$, the masses and frequencies of the decoupled oscillators are

$$M_{k\eta} = \frac{2m\sqrt{(\omega_x^2+\omega_y^2+\omega_{c\eta}^2)^2 - 4\omega_x^2\omega_y^2}}{\omega_x^2-\omega_y^2 \pm \omega_{c\eta}^2 + \sqrt{(\omega_x^2+\omega_y^2+\omega_{c\eta}^2)^2 - 4\omega_x^2\omega_y^2}}$$

$$\Omega_{k\eta} = \frac{1}{\sqrt{2}}[\omega_x^2+\omega_y^2+\omega_{c\eta}^2 \pm \sqrt{(\omega_x^2+\omega_y^2+\omega_{c\eta}^2)^2 - 4\omega_x^2\omega_y^2}]^{1/2}, \tag{5}$$

with the upper (lower) sign in $\pm$ corresponding to $k=1(2)$. We have defined in Eq. (5) a spin-dependent cyclotron frequency including the SO correction

$$\omega_{c\uparrow,\downarrow} = \frac{eB}{mc} \pm 2\lambda_D^2 \frac{m}{\hbar^3}. \tag{6}$$

The solution to Eq. (4) is given by products of x and y harmonic-oscillator functions which, when transformed back to the laboratory frame, yield the desired solutions to the original Hamiltonian of Eq. (3). The eigenvalues for each spin can be labeled according to the number of quanta in the x and y oscillators:

$$\varepsilon_{N_1N_2\eta} = \left(N_1 + \frac{1}{2}\right)\hbar\Omega_{1\eta} + \left(N_2 + \frac{1}{2}\right)\hbar\Omega_{2\eta} + s_\eta \frac{1}{2} g^* \mu_B B - \lambda_D^2 \frac{m}{\hbar^2}. \tag{7}$$

Figure 1 displays the magnetic-field evolution of the single-particle energies (7) for a circular dot, except for a constant representing the charging energy. These values give the chemical potential of the dot for a varying electron number, as measured, for instance, in capacitance spectroscopy experiments.[7,8] Actually the parabola coefficient has been taken from a fit to the experiments.[13] The spin is indicated in Fig. 1 with the light and dark gray tones. In the absence of SO coupling each line corresponds to a given spin, except for a very small fluctuation due to the Zeeman energy at some cusps and valleys. In this case the traces arrange themselves in parallel pairs of up and down spins. As shown in the two lower panels of Fig. 1, the SO coupling produces sizeable up and down fluctuations of the spin. These spin inversions are due to the level rearrangements embodied in Eq. 7. For $z_0 = 100$ Å, i.e., weak SO coupling, the fluctuations start at low magnetic fields and they extend up to $B \approx 1$ T. An even stronger SO ($z_0 = 60$ Å) produces spin inversions up to the last level crossing, which marks the filling factor $\nu = 2$ line.[13] In addition, in the latter case the traces are no longer paired but, instead, anticorrelated with a π phase shift; especially in the region just before $\nu = 2$. The results of Fig. 1 can help to interpret the experiments of Ref. 13 and Ref. 8, which observed anticorrelated behavior in the traces and spin alternation with increasing B, respectively.

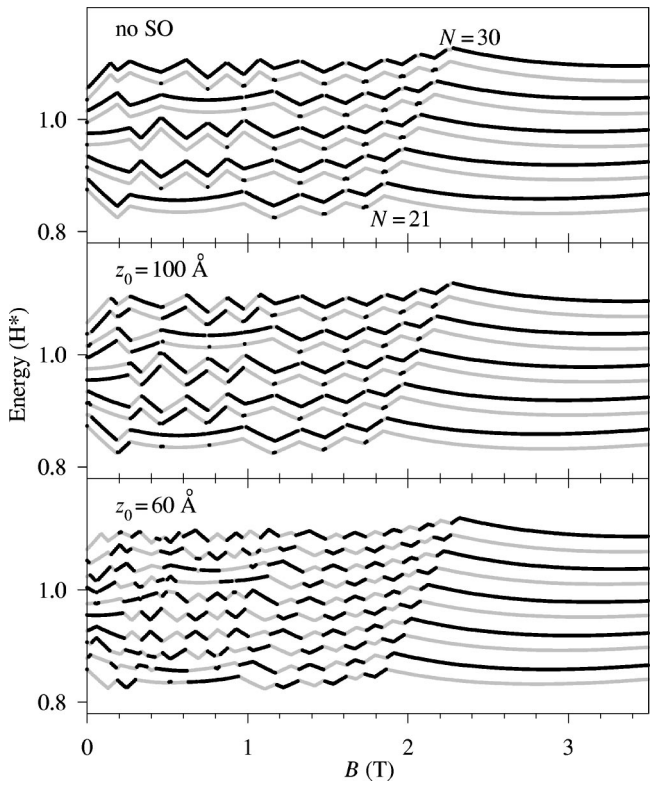

FIG. 1. Single-particle energies in modified atomic units (for GaAs $1H^* \approx 12$ meV) in the noninteracting model. Circular symmetry with $\omega_x = \omega_y = 1.1$ meV has been assumed. Each line has been shifted vertically by a small amount representing the charging energy. Light and dark gray colors correspond to up and down spins, respectively.

Having analyzed the noninteracting model we shall next estimate Coulomb interaction effects by including the self-consistent Hartree potential

$$V_H(\mathbf{r}) = \frac{e^2}{\kappa}\int d\mathbf{r}' \frac{\rho(\mathbf{r}')}{|\mathbf{r}'-\mathbf{r}|}, \tag{8}$$

where κ is the semiconductor dielectric constant ($\kappa = 12.4$ for GaAs). Electronic exchange and correlation energies will be considered using the local-spin-density approximation (LSDA) within a spinorial formalism, since $\mathcal{H}_D$ breaks the symmetry of a single spin-quantization axis. The LSDA relies on Monte Carlo calculations for the nonpolarized and fully polarized electron gases at $B = 0$.[14] A functional theory including current-density dependence, better adapted to systems in a magnetic field, is known to exist.[15] Nevertheless, current-density corrections are quite small for moderate magnetic fields and, besides, the numerical solution of the current-density-functional equations is almost unfeasible in a symmetry-unrestricted case, unless strong smoothing approximations are introduced.[16] In the results shown below we consider weak vertical magnetic fields, as quantified by the condition $\nu \geqslant 8$, where the filling factor ν is obtained from the dot central density ρ_C as $\nu = 2\pi l_B^2 \rho_C$ (with $l_B = \hbar c/eB$ the magnetic length).

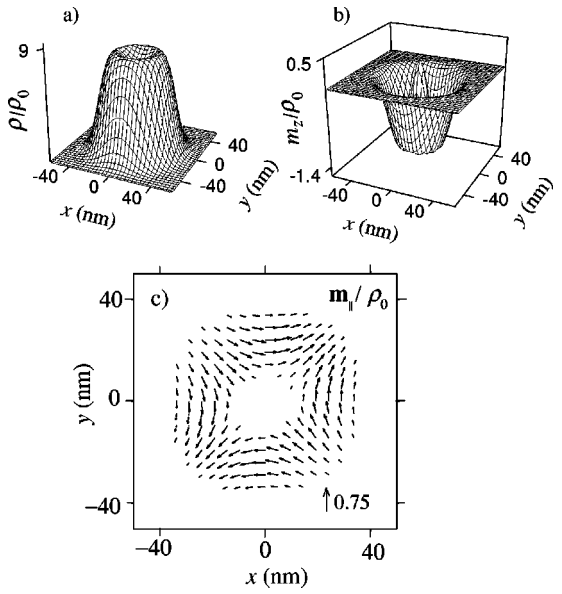

FIG. 2. Density ρ and magnetization $\mathbf{m}$ for a circular dot with $N=9$ electrons, $\hbar\omega_x=\hbar\omega_y=6$ meV, $B=2.5$ T, and $z_0=62$ Å. The values have been scaled by one-ninth of the dot central density, i.e., $\rho_0=(2.2\times10^{-5}$ Å$^{-2})/9$.

Defining the spin-density matrix in terms of the Kohn-Sham spinors $\{\varphi_i(\mathbf{r},\eta), i=1,\ldots,N\}$ as

$$\rho_{\eta\eta'}(\mathbf{r})=\sum_{i=1}^{N}\varphi_i^*(\mathbf{r},\eta)\varphi_i(\mathbf{r},\eta'), \tag{9}$$

the LSDA exchange-correlation functional $E_{xc}[\rho_{\eta\eta'}]$ yields the following 2×2 potential matrix:

$$V_{xc,\eta\eta'}(\mathbf{r})=\frac{\delta E_{xc}[\rho_{\eta\eta'}]}{\delta\rho_{\eta\eta'}(\mathbf{r})}. \tag{10}$$

Details on the evaluation of the functional derivatives in the LSDA can be found in Ref. 17. The resulting Kohn-Sham equations read

$$\left[\frac{\mathbf{P}^2}{2m}+\frac{1}{2}m(\omega_x^2x^2+\omega_y^2y^2)+s_\eta\frac{1}{2}g^*\mu_BB+V_H(\mathbf{r})\right]\varphi_i(\mathbf{r},\eta)$$
$$+\sum_{\eta'}\left[\frac{\lambda_D}{\hbar}(P_x\sigma_x-P_y\sigma_y)_{\eta\eta'}+V_{xc,\eta\eta'}(\mathbf{r})\right]\varphi_i(\mathbf{r},\eta')$$
$$=\varepsilon_i\varphi_i(\mathbf{r},\eta). \tag{11}$$

We have solved Eqs. (11) by discretizing the xy plane in a uniform grid of points and applying an iterative scheme to reach full self-consistency in $V_H(\mathbf{r})$ and $V_{xc,\eta\eta'}(\mathbf{r})$. In some cases this procedure might get trapped in a local minimum. Therefore, several calculations with different random initial conditions have to be used to ensure that the proper energy minimum is reached. The stability with the number of mesh points has also been checked.

Figure 2 displays the density $\rho(\mathbf{r})$ and spin magnetization $\mathbf{m}(\mathbf{r})$ for $N=9$ electrons in a circular confining potential with $\omega_x=\omega_y=6$ meV. We have selected this electron number as a representative case of where to check the robustness of the analytically predicted spin inversions. A SO coupling with $z_0=62$ Å and $B=2.5$ T have been assumed. The magnetization density indicates the local orientation of the spin vector and it is related to the spin-density matrix by $m_x=2\,\mathrm{Re}[\rho_{\uparrow\downarrow}]$, $m_y=2\,\mathrm{Im}[\rho_{\uparrow\downarrow}]$, and $m_z=\rho_{\uparrow\uparrow}-\rho_{\downarrow\downarrow}$. We note from Fig. 2 that circular symmetry is conserved by both ρ and m_z, while the horizontal magnetization $\mathbf{m}_\parallel\equiv(m_x,m_y)$ shows an angular dependent texture. This result is in good agreement with the analytical solution given above, that predicts $\mathbf{m}_\parallel(\mathbf{r})\sim\rho(r)$ (y,x). Note also that for this particular z_0 and B the vertical spin is predominantly inverted, giving a negative value for the total vertical spin $\langle S_z\rangle$.

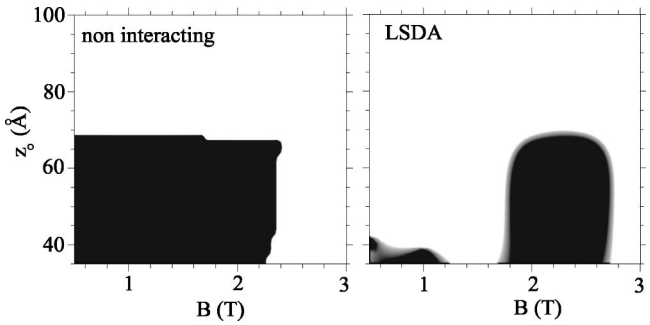

FIG. 3. Vertical spin evolution in the B-z_0 plane for the same quantum dot of Fig. 2. White (black) color indicates upward (downward) total spin.

Figure 3 shows $\langle S_z\rangle$ as a function of B and the intensity of the SO coupling, given by z_0, for the same dot of Fig. 2. In agreement with the above discussion, for $B\leqslant2.2$ T the noninteracting model predicts spin inversion when decreasing the dot width. The LSDA also yields spin-inverted regions although with some conspicuous differences that can be attributed to a higher rigidity in the electronic structure. The interaction inhibits the spin flip at low magnetic fields and low widths, shifting the inversion region to $1.8\,\mathrm{T}\leqslant B\leqslant2.6$ T and leaving only a small residue for $z_0\leqslant40$ Å and $B\leqslant1.2$ T. It is worth mentioning that although in the laboratory frame $\langle S_z\rangle$ is not restricted to discrete values (because of the transformation U_1), in practice its fluctuations increase with the SO strength but they are generally small. In Fig. 3 the deviations from $\pm\hbar/2$ when $z_0=62$ and 48 Å are $\approx5\%$ and $\approx20\%$, respectively. Experimentally the dot width can be controlled with the electric gates; therefore, the results of Fig. 2 suggest a spin switch behavior, controllable with vertical magnetic and electric fields.

In Fig. 4 we show the vertical spin as a function of the applied magnetic field and the dot deformation, for two different values of the SO coupling. In this figure the mean value $(\omega_x+\omega_y)/2$ was kept fixed to 6 meV while the ratio $\delta=\omega_y/\omega_x$ was varied to obtain different elliptical shapes. Comparing left and right panels we see again an interaction-induced quenching of the spin inversion at low magnetic fields. Although this occurs for the two displayed widths, at $z_0=48$ Å a larger region with inverted spin is found. Figure 4 shows that, having fixed the SO coupling strength, spin inversion can be achieved in many cases either by increasing

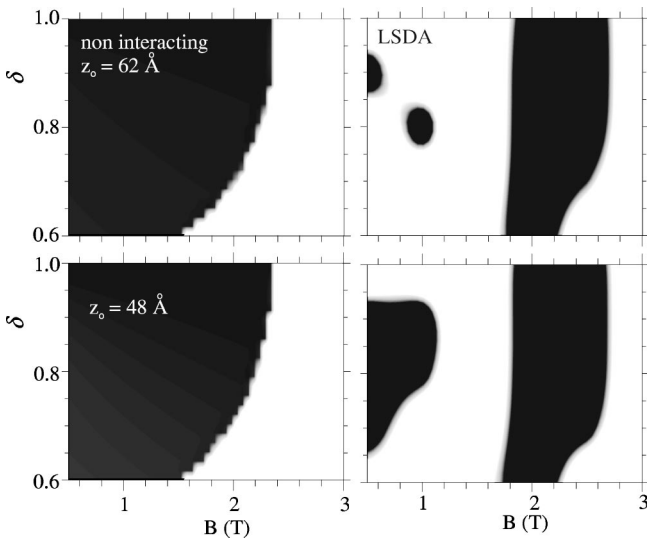

FIG. 4. Vertical spin evolution in the B-δ plane, where $\delta = \omega_y/\omega_x$ labels the deformation, for a fixed value of the SO coupling. Upper row corresponds to $z_0 = 62$ Å in the noninteracting model (left) and the LSDA (right). Lower row shows the same results for $z_0 = 48$ Å. We have used the same color convention of Fig. 3.

the deformation or, alternatively, by increasing the magnetic field. The comparison of the $N=9$ numerical results with the analytical model allows us to conclude that, in spite of the differences, the spin inversions in the LSDA are qualitatively similar to the analytical ones. More specifically, both models display inversions in the same range of magnetic fields, SO strengths, and deformations. As a final piece of information that we mention is that the energy gap between the highest occupied and lowest unoccupied Kohn-Sham levels in the above cases stays in the range [0.3, 0.9] meV. This result provides a measure of the ground state stability and, therefore, of the relative spin stiffness against thermal fluctuations.

In summary, the mechanism of spin switch through SO coupling has been analyzed. It has been shown that SO coupling can lead to anticorrelated behavior in the B evolution of neighboring levels and to up- and down-spin oscillations, qualitatively similar to experimental observations. The combined effects of SO coupling, weak magnetic fields, and deformation have been studied, first analytically with a noninteracting model, and second, by taking into account interaction effects within the LSDA. The diagrams with the spin dependence on these parameters suggest the characterization of the quantum dots as spin switches, of relevance to spintronic technology.

This work was supported by Grant No. BFM2002-03241 from DGI (Spain), and by COFINLAB from Murst (Italy).

[1] S. A. Wolf, D. D. Awschalom, R. A. Buhrman, J. M. Daughton, S. von Molnár, M. L. Roukes, A. Y. Chtchelkanova, and D. M. Treger, Science **294**, 1488 (2001).
[2] S. Datta and B. Das, Appl. Phys. Lett. **56**, 665 (1990).
[3] J. A. Folk, S. R. Patel, K. M. Birnbaum, C. M. Marcus, C. I. Duruöz, and J. S. Harris, Phys. Rev. Lett. **86**, 2102 (2001).
[4] B. I. Halperin, A. Stern, Y. Oreg, J. N. H. J. Cremers, J. A. Folk, and C. M. Marcus, Phys. Rev. Lett. **86**, 2106 (2001).
[5] I. L. Aleiner and V. I. Fal'ko, Phys. Rev. Lett. **87**, 256801 (2001).
[6] M. Valín-Rodríguez, A. Puente, and Ll. Serra, Phys. Rev. B **66**, 045317 (2002).
[7] R. C. Ashoori, Nature (London) **379**, 413 (1996), and references therein.
[8] M. Ciorga, A. S. Sachrajda, P. Hawrylak, C. Gould, P. Zawadzki, S. Jullian, Y. Feng, and Z. Wasilewski, Phys. Rev. B **61**, R16 315 (2000).
[9] O. Voskoboynikov, C. P. Lee, and O. Tretyak, Phys. Rev. B **63**, 165306 (2001).
[10] We assume the symmetric gauge to relate the vertical magnetic field and the vector potential as $\mathbf{A} = B/2(-y,x)$.
[11] W. Knap, C. Skierbiszewski, A. Zduniak, E. Litwin-Staszewska, D. Bertho, F. Kobbi, J. L. Robert, G. E. Pikus, F. G. Pikus, S. V. Iordanskii, V. Mosser, K. Zekentes, and Yu. B. Lyanda-Geller, Phys. Rev. B **53**, 3912 (1996).
[12] H. D. Meyer, J. Kucar, and L. S. Cederbaum, J. Math. Phys. **29**, 1417 (1988).
[13] R. C. Ashoori, H. L. Stormer, J. S. Weiner, L. N. Pfeiffer, K. W. Baldwin, and K. W. West, Phys. Rev. Lett. **71**, 613 (1993).
[14] B. Tanatar and D. M. Ceperley, Phys. Rev. B **39**, 5005 (1989).
[15] G. Vignale and M. Rasolt, Phys. Rev. B **37**, 10 685 (1988); M. Ferconi and G. Vignale, *ibid.* **50**, 14 722 (1994).
[16] M. Koskinen, J. Kolehmainen, S. M. Reimann, J. Toivanen, and M. Manninen, Eur. Phys. J. D **9**, 487 (1999).
[17] O. Heinonen, J. M. Kinaret, and M. D. Johnson, Phys. Rev. B **59**, 8073 (1999).